Dark Aerobic Growth Conditions Induce the Synthesis of a High Midpoint Potential Cytochrome c_8 in the Photosynthetic Bacterium *Rubrivivax gelatinosus*

Laure Menin,[‡] Makoto Yoshida,[§] Michel Jaquinod,[||] Kenji V. P. Nagashima,[§] Katsumi Matsuura,[§] Pierre Parot,[‡] and André Verméglio*[,‡]

C.E.A./Cadarache-DSV-DEVM-Laboratoire de Bioénergétique Cellulaire, 13108 Saint-Paul-lez-Durance Cedex, France, Department of Biology, Tokyo Metropolitan University, Minamiohsawa 1−1, Hachioji, Tokyo 192-0397, Japan, LSMP, CEA/CNRS, Institut de Biologie Structurale, 41, avenue Jules-Horowitz, 38027 Grenoble Cedex, France.

Received May 18, 1999; Revised Manuscript Received September 8, 1999

ABSTRACT: In several strains of the photosynthetic bacterium *Rubrivivax gelatinosus*, the synthesis of a high midpoint potential cytochrome is enhanced 4−6-fold in dark aerobically grown cells compared with anaerobic photosynthetic growth. This observation explains the conflicting reports in the literature concerning the cytochrome *c* content for this species. This cytochrome was isolated and characterized in detail from *Rubrivivax gelatinosus* strain IL144. The redox midpoint potential of this cytochrome is +300 mV at pH 7. Its molecular mass, 9470 kDa, and its amino acid sequence, deduced from gene sequencing, support its placement in the cytochrome c_8 family. The ratio of this cytochrome to reaction center lies between 0.8 and 1 for cells of *Rvi. gelatinosus* grown under dark aerobic conditions. Analysis of light-induced absorption changes shows that this high-potential cytochrome c_8 can act in vivo as efficient electron donor to the photooxidized high-potential heme of the *Rvi. gelatinosus* reaction center.

The conversion of light into chemical energy by photosynthetic organisms is initiated by a light-induced charge separation at the reaction center (RC).[1] In the case of purple bacteria, this charge separation is followed by a cyclic electron transfer, coupled to the formation of a transmembrane electrochemical gradient used for NAD^+ reduction and ATP production. This light-induced cyclic electron-transfer involves, in addition to the RC, the cytochrome (cyt) bc_1 complex, quinone molecules, and periplasmic soluble electron carriers. For most photosynthetic Proteobacteria, the direct reductant of the RC photooxidized primary electron donor is an RC-bound cyt *c* containing two high-potential (HP) and two low-potential (LP) hemes (*1*). The chemical nature of the periplasmic carriers, which mediate electron transfer between the RC and the cyt bc_1 complex, depends on the species (*2*). It can be either a *c*-type cyt (cyt c_2 or cyt c_8) or a high-potential iron−sulfur protein (HiPIP). *c*-type cytochromes possess a typical heme attachment sequence motif (-Cys-X-Y-Cys-His-). Cyts c_2 are larger than cyts c_8 by several extra loops (*3*). Cyts c_8 are characterized by two to four proline residues around the sixth ligand methionine and a conserved tryptophane residue near the C-terminus (*4*). In photosynthetic bacteria, the presence of cyts c_8 has only been described for species possessing an RC-bound tetraheme cyt, and it was proposed that they might function in a manner similar to the cyt c_2 in connecting the RC and the cyt bc_1 complex (*5*). HiPIPs form a class of small proteins containing a cubane $[Fe_4S_4]^{3+/2+}$ redox couple found in several photosynthetic and nonphotosynthetic representatives of Proteobacteria.

Rubrivivax (Rvi.) gelatinosus is a non-sulfur phototrophic bacterium of the β subclass of Proteobacteria. The RC of *Rvi. gelatinosus* contains an RC-bound cyt *c* with two HP ($E_{m,7}$ = 300 and 320 mV) and two LP hemes ($E_{m,7}$ = 70 and 130 mV) (*6*, *7*). Several soluble electron carriers have been found in the periplasmic space of *Rvi. gelatinosus.* A low-potential cyt c_8, cyt *c*-551, or LP cyt c_8 ($E_{m,7}$ = + 30 mV) and a cyt c' ($E_{m,7}$ = + 55 mV) are present in different strains of *Rvi. gelatinosus* (*5*, *8*). In vitro experiments have shown that the LP cyt c_8 and the cyt c' act as electron donors to the photooxidized primary electron donor in a *Rvi. gelatinosus* mutant (C244) deleted in RC-bound tetraheme cyt (*9*). The LP cyt c_8 is also a good electron donor to the RC-bound tetraheme cyt of the wild-type strain of *Rvi. gelatinosus* IL144 (*9*), but owing to its low midpoint potential, it cannot be involved in the photoinduced cyclic electron transfer. HiPIP has been found in all strains of *Rvi. gelatinosus* studied so far. This carrier has been characterized in terms of E_m (+330 mV) (*10*) and amino acids sequence (*11*). According to Meyer (*12*), HiPIP is the only high-potential soluble carrier present in the periplasmic space of *Rvi. gelatinosus* ATH 2.2.1. This early observation agrees with recent in vivo experiments that have shown that the HiPIP is the carrier that mediates electron transfer between the photooxidized RC-bound HP heme(s) and the cyt bc_1 complex (*13*) in photosynthetically grown cells of this species. However, the presence, in *Rvi. gelatinosus* cells, of

* To whom correspondence should be addressed. Phone: 33 442254630. Fax: 33 442254701. E-mail: AVermeglio@cea.fr.

[‡] C.E.A./Cadarache-DSV-DEVM-Laboratoire de Bioénergétique Cellulaire.

[§] Tokyo Metropolitan University.

[||] Institut de Biologie Structurale.

[1] Abbreviations: cyt, cytochrome; E_m, redox midpoint potential; HiPIP, high-potential iron−sulfur protein; HP, high potential; LP, low potential; MALDI-MS, matrix-assisted laser desorption ionization−mass spectrometry; PS, photosynthetic; RC, reaction center; *Rcy.*, *Rhodocyclus*; *Rfx.*, *Rhodoferax*; *Rvi.*, *Rubrivivax*.

10.1021/bi991146h CCC: $18.00
Published on Web 10/29/1999

a periplasmic, diheme, high-potential cyt c_4 of about 20 kDa has been noted (*3*). Evidence for the presence of a HP cyt *c* has also been reported by Matsuura et al. (*14*) for strain IL144 of *Rvi. gelatinosus*. Although the redox properties of this cyt were not described in detail, reconstitution experiments have shown that it can act as an efficient electron donor to the HP heme of the tetraheme cyt *c*. More recently, a HP cyt *c* ($E_{m,7} = +294$ mV) was isolated and characterized from cells of *Rvi. gelatinosus* strain 1709 by Borsari et al. (*15*). It is therefore possible that the presence of a HP cyt *c* in *Rvi. gelatinosus* depends on the strains considered.

To clarify this point, an analysis of the periplasmic content in electron carriers by biophysical and biochemical means was performed for three different strains of *Rvi. gelatinosus*. Our results show that the synthesis of a HP cyt *c* is enhanced under dark aerobic growth conditions. We describe the purification and characterization of this cyt.

MATERIALS AND METHODS

Bacterial Growth. Three different strains, IL144 (*16*), TG-9 (*17*), and ATCC 17011 (or S1) (*18*), of *Rvi. gelatinosus* were used in this study. Cells were grown in Hutner medium for either anaerobic photosynthetic (PS) or dark aerobic conditions. For PS growth, the bacteria were illuminated by incandescent lightbulbs (75 μmol of photons m^{-2} s^{-1}) in 100 mL anaerobic medium at 30 °C. For aerobic cultures, 500 mL conical flasks containing 200 mL of medium were shaken in the dark (200 rpm, 28 °C). In both cases, the innoculum was 5% and the cells were harvested after 24 h.

Preparation of the Periplasmic Fraction. The periplasmic fraction was prepared as described by Sabaty et al. (*19*). *Rvi. gelatinosus* cells were washed with 50 mM Tris-HCl (pH 8) and resuspended in the same buffer in the presence of 0.45 M sucrose, 1.3 mM EDTA, and 1 mg/mL lysozyme. After 2 h of incubation at 30 °C, the suspension was spun down for 20 min at 4000*g* (rotor JA-20, Beckman model J2-21). The supernatant constitutes the periplasmic fraction.

Gel Electrophoresis. SDS−PAGE was performed with a Mini Protean apparatus (Bio-Rad). The resolving gel contained 15% acrylamide. Heme staining was performed by incubation in 3,3′,5,5′-tetramethylbenzidine (TMBZ) with visualization by hydrogen peroxide as previously described (*20*).

Purification of the Periplasmic Electron Carriers. All the experiments were performed at 4 °C. The pH of the periplasmic fraction was adjusted to 6 before ultracentrifuging for 1 h and 30 min at 200000*g* (rotor 70Ti, Beckman model L8-M). The supernatant was dialyzed against 20 mM Tris-HCl (pH 6) for one night and loaded on a cellulose CM-23 column (Whatman) equilibrated with the same buffer. A stepwise salt gradient was applied on the column. The HiPIP, the HP cyt c_8, the LP cyt c_8, and the cyt c' were eluted with 25, 45, 65, and 80 mM NaCl, respectively. Fractions corresponding to these different electron carriers were separately pooled. Each pool was then concentrated to 1 mL by ultrafiltration with a PM5000 membrane (Millipore) and applied to a Sephadex G-100 column (Pharmacia) equilibrated with 20 mM Tris-HCl pH 6. This last step was repeated to obtain the purest fractions of the HP cyt c_8.

Redox Titrations. Redox titrations were performed in 20 mM Tris-HCl (pH 7) with the following mediators: *p*-benzoquinone, 10 μM; diaminodurene, 50 μM; 1,2-naphthoquinone, 20 μM; phenazine methosulfate, 20 μM; duroquinone, 20 μM; and 2-OH-1,4-naphthoquinone, 20 μM. The ambient redox potential (E_h), measured with a combined Ag/AgCl reference system electrode (Mettler Toledo), was adjusted by addition of small aliquots of potassium ferricyanide (10 mM), sodium ascorbate (10 mM), or dithionite (10 mM). The concentration of reduced cyt, as a function of E_h, was determined by measuring the optical density at 550 nm using a U-2000 spectrophotometer (Hitachi). Experimental data were fitted with ($n = 1$) Nernst curves using the Sigmaplot program (Jandel Scientific).

Amino Acid Sequencing. Amino acid sequencing was performed using an automatic sequencer (Applied Biosystems 477A) with the sample blotted on PVDF membrane (Applied Biosystems).

Mass Spectroscopy. Matrix-assisted laser desorption ionization−mass spectra (MALDI-MS) were recorded on a Voyager-Elite XL Biospectrometry workstation (Perspective BioSystems, Inc., Framingham, MA). The matrix was 2,5-dihydroxybenzoic acid purchased from Sigma. One microgram of the HP cyt c_8 (5 pmol/μL) dissolved in an aqueous solution of acetate ammonium buffer 10 mM (pH 7.5) was mixed with 1 μL of the saturated solution of matrix in 50% CH_3CN/0.1% trifluoroacetic acid (Sigma). One microliter of this mixture was deposited on the target and dried. Spectra were recorded from 256 laser shots (nitrogen laser, 337 nm) with an accelerating voltage of 20 000 V in the linear mode. The other parameters were grid voltage, 94.7%; guide wire voltage, 0.1%; and pulse source delay time, 150 ns. The instrument was calibrated using human insulin (Boehringer Mannheim, Mannheim, FRG).

Cloning and Sequencing of HP Cyt c_8 Gene. A DNA fragment containing part of the gene coding for the HP cyt c_8 was amplified by polymerase chain reaction (PCR) using the primers GHPC551F (5′-GCSCCSGARGACATCGTSAA) designed based on the N-terminal amino acid sequence of the purified HP cyt c_8 of *Rvi. gelatinosus* IL144 and GHPC551R (5′-CCCTCRCCRCCSGCCATSACCTT) based on the known amino acid sequences of cyts c_8 of various purple bacteria. PCR was performed using a GeneAmp PCR Kit (Perkin-Elmer) in a Zymoreacter (ATTO, Japan) as described previously (*21*). The PCR product was labeled by digoxigenin using a DIG-High Prime kit (Boehringer Mannheim) and was used as a probe for screening of the cosmid library of *Rvi. gelatinosus* IL144 genomic DNA (*22*). A positive clone was detected and denominated pGHC1cos. The purified pGHC1cos cosmid DNA was digested with a restriction enzyme, *Sma*I, and subcloned into pHSG396 plasmids at the unique *Hinc*II site in the multicloning site. A clone, pGHC1, was screened by hybridization with the same probe used in the cosmid screening. The 1164 bp insert DNA fragment of pGHC1 containing a gene for HP cyt c_8 was sequenced using a Dye Terminator Cycle Sequencing Kit and a Prism 310 genetic Analyzer (PE Applied Biosystems). Nucleotide sequence data was analyzed by a software package of DNASIS (Hitachi soft, Japan) and has been submitted to the DDBJ, EMBL, and GenBank with an accession number of AB030281.

Light-Induced Absorption Changes on Intact Cells. Light-induced absorption changes were measured with a laboratory-built spectrophotometer as described previously (*13*). The

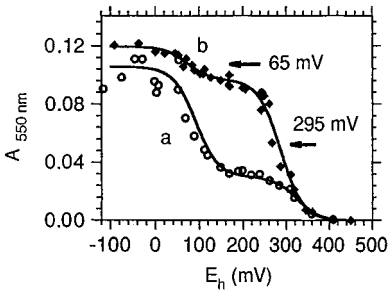

FIGURE 1: Redox titrations of the periplasmic fractions of *Rvi. gelatinosus* IL144 cells grown under PS conditions (curve a, ○) or aerobically in the dark (curve b, ◆). Experimental data were obtained by monitoring the absorbance at 550 nm as a function of the imposed E_h. The solid line represents the best fit of the data to the sum of two ($n = 1$) Nernst equation components. Mediators: *p*-benzoquinone, 10 μM; diaminodurene, 50 μM; 1,2-naphthoquinone, 20 μM; phenazine methosulfate, 20 μM; duroquinone, 20 μM; and 2-OH-1,4-naphthoquinone, 20 μM. Buffer: Tris-HCl 20 mM (pH 7).

cells were resuspended in fresh growth medium made anaerobic by bubbling through nitrogen. A weak background illumination, provided by a 24 V quartz lamp filtered through two Kodak Wratten 89B red filters (1.25 W m^{-2}), was applied to specifically accumulate the photooxidized state of LP hemes of the RC-bound cyt (see Results for details).

RESULTS

Periplasmic Fraction Analysis. The periplasmic fractions of *Rvi. gelatinosus* cells grown under PS or dark aerobic conditions were isolated as described in the Materials and Methods. To determine and compare their relative cyt contents, we recorded the absorption at 550 nm, a typical α−band wavelength of reduced cyt *c*, as a function of the ambient redox potential (E_h). Figure 1 shows typical potentiometric titrations for the periplasmic fractions of strain IL144. For both PS (curve a) or dark aerobic (curve b) growth conditions, the titration curves present two distinct components that can be simulated by two ($n = 1$) Nernst curves using E_ms of +65 and +295 mV. We attribute the low-potential component to the contribution of the LP cyt c_8. The second component is tentatively attributed to the reduction of a HP cyt *c*. One interesting observation is that the relative amplitudes of the two components, i.e., the relative amounts of the high and low midpoint potential cyts *c*, depend closely on the growth conditions. For PS grown cells, the HP component corresponds to less than 30% of the total amount of soluble cyt *c*, against more than 80% for aerobically grown cells. Similar results were obtained for strains TG9 and ATCC 17001 of *Rvi. gelatinosus* (data not shown). We have characterized in more detail this HP component in the case of *Rvi. gelatinosus* IL144. Reduced (dithionite) minus oxidized (ferricyanide) difference spectra of the soluble and membrane fractions of cells of *Rvi. gelatinosus* were used to determine the relative ratio of RC-bound cyt *c* to these two soluble cyts *c* (data not shown). We found between 0.8 and 1 HP cyt *c*/RC for cells grown under dark aerobic conditions. This ratio lay between 0.15 and 0.2 for PS grown cells. There is about 0.2 and 0.5 LP cyt c_8/RC for cells grown under dark aerobic or PS conditions, respectively. The cyt content was also analyzed by SDS−PAGE and specific staining of the hemes (Figure 2). Despite the large difference in the amounts of LP and

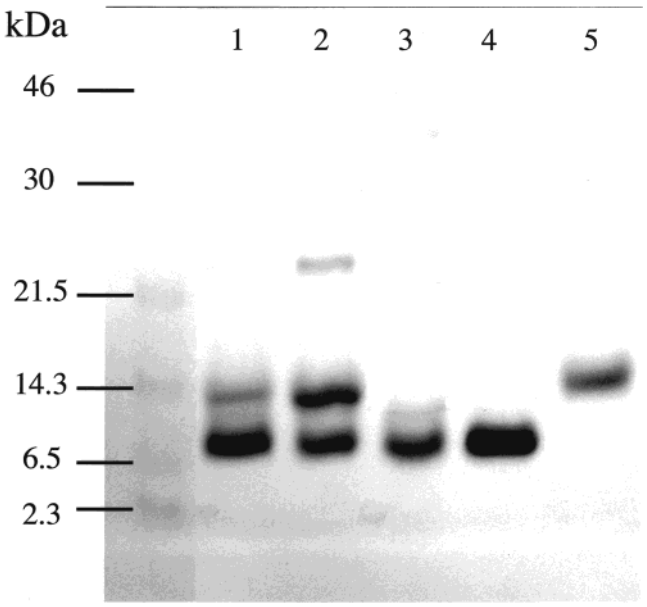

FIGURE 2: SDS−PAGE at 15% of periplasmic fractions of dark aerobically (lane 1) and PS (lane 2) grown cells of *Rvi. gelatinosus* IL144. Lanes 3, 4, and 5 correspond to purified LP c_8, HP cyt c_8, and cyt c′, respectively. The gel was stained for heme.

HP cyts *c* for PS or dark aerobically grown cells, the pattern of the heme bands is very similar for the two periplasmic fractions (compare lanes 1 and 2 of Figure 2). Two major bands are observed with apparent molecular masses around 14 and 10 kDa. The main difference between the two growth conditions is the relative importance of these two bands, the 14 kDa band being more intense under PS than under dark aerobic growth conditions. Comparison with the electrophoretic behavior of purified cyt *c*′ (lane 5) shows that the 14 kDa band corresponds to cyt *c*′. The presence of a higher concentration of cyt *c*′ under PS growth conditions compared with dark aerobic condition was confirmed by absorption spectroscopy (data not shown). Both purified LP cyt c_8 (lane 3) and HP cyt *c* (lane 4) present an apparent molecular mass of about 10 kDa. The very similar electrophoretic mobility of the LP cyt c_8 and the HP cyt *c* (see below) explains why no clear-cut difference is observed for the cyt pattern of periplasmic fractions of PS and dark aerobic growth conditions (Figure 2, lanes 1 and 2) despite their large difference in cyt content. Numerous attempts were made to separate these two cyts by gel isoelectrofocusing. We failed mainly because these two cyts are highly basic (pI > 9.5) and their pI values are very close. The predicted pI values from the amino acid sequences (see below and ref *22*) of these cyts are 9.79 and 10.07 for the HP cyt *c* and for the LP cyt c_8, respectively.

Purification and Characterization of the High Midpoint Potential Cyt c. To better characterize the HP cyt *c*, this electron carrier was purified from the periplasmic fraction of dark aerobically grown cells of *Rvi. gelatinosus* IL144. The purification was performed in two steps using cellulose CM-23 and Sephadex G-100 columns. The final purity of the protein was monitored by gel electrophoresis and UV−vis spectroscopy. For the purest fractions, the absorbance A_{280}/A_{415} was 0.30. The absorption spectrum of the purified protein was typical of cyt *c* with maxima at 550 nm (α), 521 nm (β), and 418 nm (γ) in the reduced state. Oxidation−

Table 1: Amino Acid Sequence Alignment of Soluble Cytochromes from Different Strains of *Rvi. gelatinosus*[a]

```
                                          10        20        30        40        50
1. Rvi. gelatinosus IL144 HP c8             MIKPLLAALGLAVVSASALAAPEDIVKKSGCLACHQVDKKVVGPSYKEVA
2. Rvi. gelatinosus IL144 LP c8           MNRTVSRLALAAGLVFGAAATHAATPAELATKAGCAVCHQPAAKGLGPSYQEIA
3. Rvi. gelatinosus ATCC 17011                        ATPAELATKAGCAVCHQPTAKGLGPSYQEIA
4. Rvi. gelatinosus 29-1 iso-1                        ATPAELATKAGCAVCHQPAAKVLGPSY....
5. Rvi. gelatinosus 29-1 iso-2                         APEDIVKKSGCLMCHGVDKKVSGPSY....
                                        60        70        80        90        100
1. Rvi. gelatinosus IL144 HP c8          AKYKGKK-ADAQLFDKVRKGGGGVWGPIPMIPHTPQQISDADLKTVITWILAQ
2. Rvi. gelatinosus IL144 LP c8          KKYKGQAGAPATMAERVRKGSVGVFGKVPMTPTPPARISDADLKTVIDWILKTP
3. Rvi. gelatinosus ATCC 17011           KKYKGQAGAPALMAERVRKGSVGIFGKLPMTPTPPARISDADLKLVIDWILKTP
```

[a] (1) This work. (2) Ref *22*. (3) Ref *3*. (4, 5) Ref *28*. the amino acid sequences of 1 and 2 are based on the nucleotides sequences. The amino acid sequence determined from the purified HP cyt c_8 of *Rvi. gelatinosus* IL144 is underlined.

reduction of the purified cyt, followed at 550 nm, closely fitted the Nernst equation for a single $n = 1$ component with a midpoint potential of +300 mV at pH 7 (data not shown), in agreement with the value obtained for one component of the periplasmic fractions. The MALDI-MS spectrum of this cyt indicates a homogeneous population. The peaks of the 2^+ and 1^+ charged states of the protein correspond to a molecular mass of 9472 ± 2 Da (data not shown). The sequence of 20 amino acids of the N-terminus of the HP cyt *c* has been determined by microsequencing. The gene coding for this cyt has been sequenced from a cosmid library of *Rvi. gelatinosus* as described in the Materials and Methods. The deduced product of this HP cyt gene is composed of 102 amino acid residues (Table 1). The 20 amino acids from the N-terminus appear to be a signal peptide since the purified protein lacks this part. The calculated molecular mass of the mature HP cyt is 9470 Da when taking into account processing of the peptide signal and binding of a *c*-type heme in very good agreement with the MALDI-MS experiments. The deduced amino acid sequence clearly indicates that this HP cyt belongs to the class of small *Pseudomonas* cyt *c*-551 designated cyt c_8 by Ambler (*4*). The amino acid sequence of the HP cyt c_8 is distinct from that of the LP cyt c_8, showing a sequence identity of only 55% (Table 1). The significant difference in midpoint potential and in amino acid sequence between this cyt and the LP cyt c_8 (*22*) demonstrates the occurrence of two distinct cyts c_8 in *Rvi. gelatinosus*. In the 129 bp upstream region of the gene for the HP cyt c_8, an open reading frame (ORF) showing 75% sequence identity to the 3′-region of the *nirN* gene of *Pseudomonas aeruginosa* which is a member of *nir* gene cluster necessary for production of dissimilatory nitrite reductase (*23*) was detected on the same strand with the HP cyt c_8 gene. In *P. aeruginosa*, the cyt c_8 (c-551) is coded by *nirM* gene (*24*) and serves as a physiological electron donor for the nitrite reductase (*25*). In the downstream region of the HP cyt c_8 gene of *Rvi. gelatinosus*, an ORF showing 62% sequence identity to the 3′-region of the *E. coli* map gene coding for a methionine aminopeptidase was located on the complementary strand.

Light-Induced Absorption Changes in Intact Cells. The cyt characterized above corresponds certainly to the HP cyt that acts as an efficient electron donor to the HP heme of the RC-bound tetraheme cyt *c* in reconstitution experiments (*14*). This prompted us to determine whether the HP cyt c_8 could be an efficient electron donor to the HP hemes of the RC-bound tetraheme cyt in vivo for *Rvi. gelatinosus* cells grown under dark aerobic conditions. We therefore compared light-induced absorption changes in intact cells of *Rvi. gelatinosus* grown under dark aerobic and PS conditions. When PS grown cells are assayed under anaerobic conditions, a saturating flash induces the photooxidation of the LP heme

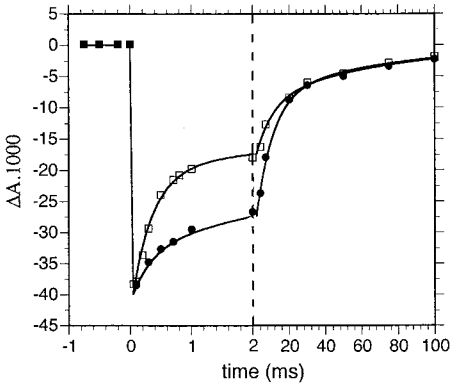

FIGURE 3: Kinetics of tetraheme cyt HP heme rereduction measured at 422 nm on whole cells of *Rvi. gelatinosus* IL144 ([RC] = 480 nM) grown under PS (□) and dark aerobic conditions (●). Note the two different time scales. Cells were placed under anaerobic conditions and subjected to a weak illumination of 1.25 W m^{-2} to photooxidize the LP hemes of the RC-bound tetraheme cyt.

followed by its very slow rereduction (*13*). Similar behavior was observed for cells grown under dark aerobic conditions (data not shown). The photooxidation of the RC-bound HP hemes can only occur after photooxidation of the two LP hemes (*13*). This can be achieved by preillumination by two saturating flashes or by the superimposition of a weak continuous illumination onto the actinic flash (*26*). Kinetics of HP heme photooxidation and reduction, detected at 422 nm under the latter condition, are shown in Figure 3 for PS or dark aerobically grown cells of *Rvi. gelatinosus*. The rereduction kinetics are multiphasic for both growth conditions. They can be decomposed into three exponentials with respective halftimes of about 240 μs, 7 ms, and 50 ms. The relative amplitudes of these phases are highly dependent on the growth conditions. In particular, the 240 μs phase represents more than 50% for PS grown cells, but less than 15% for dark aerobically grown cells. A detailed study on *Rvi. gelatinosus* cells grown under PS condition has already shown that this 240 μs phase is related to the rereduction of the photooxidized HP heme by the HiPIP (*13*). Two hypotheses could explain the small amplitude of this phase for cells grown under dark aerobic conditions compared with PS grown cells (Figure 3). First, HiPIP is present in small concentrations in these dark aerobic growth conditions. Second, an electron donor, with an optical contribution at 422 nm, is acting as secondary electron donor in these cells. To test the first hypothesis, we measured, by combining EPR and absorption spectroscopies, the ratio of HiPIP to RC for *Rvi. gelatinosus* cells grown under PS or dark aerobic conditions. This ratio was found to be similar, 1.3−2 HiPIP molecules/RC, in each of the growth conditions. To show

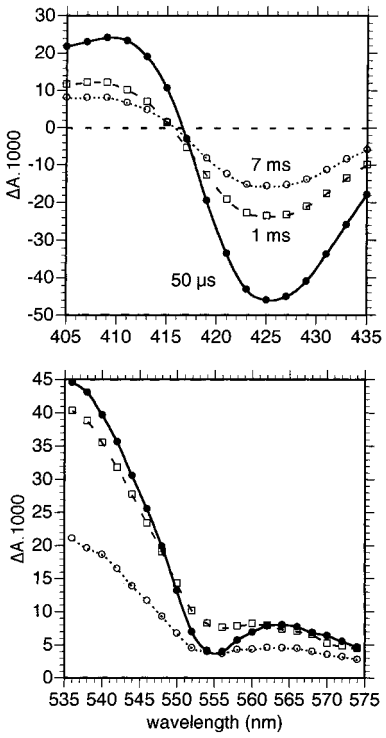

FIGURE 4: Light-induced absorption changes measured in the Soret and the α-band region for intact cells of *Rvi. gelatinosus* IL144 grown under PS condition ([RC] = 500 nM). The intact cells were placed under anaerobic conditions and subjected to a weak illumination of 1.25 W m^{-2} to photooxidize the LP hemes of the RC-bound tetraheme cyt. The absorption changes were sampled at discrete times (50 μs, ●; 1 ms, □; 7 ms, ○) after the actinic flash. The absorption changes in the 535−545 nm region are due to the carotenoid bandshift.

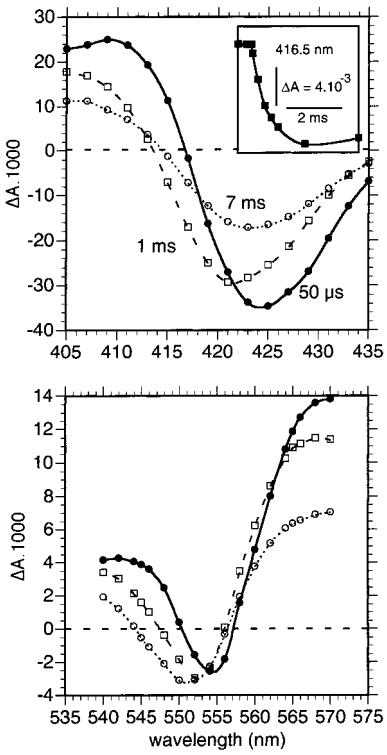

FIGURE 5: Same as Figure 6 but for dark aerobically grown cells of *Rvi. gelatinosus* IL144 ([RC] = 550 nM). The absorption changes in the 560−570 nm are due to the carotenoid band shift. Dark aerobic growth condition induces the formation of oxidized forms of carotenoid absorbing in this spectral range. (Inset) Kinetics of electron transfer between the soluble HP cyt c_8 and the photooxidized RC-bound HP heme recorded at 416.5 nm.

the participation of different electron carriers in each of the growth conditions, we measured light-induced difference spectra at different times after the actinic flash in the γ- and α-band regions. For cells of *Rvi. gelatinosus* grown under the PS condition (Figure 4), the photooxidized RC-bound HP heme, with characteristic bleaching peaking at 554 and 425 nm, is rapidly rereduced. This reduction step, which corresponds to the fast phase observed at 422 nm (Figure 3) is not accompanied by the appearance of any new component in the light-induced difference spectra (Figure 4, see also Figure 5 of ref *13*). As already stated, this observation was evidence that HiPIP is the electron donor to the photooxidized RC-bound HP heme (*13*). The situation is completely different for cells grown under dark aerobic condition (Figure 5). The photooxidation of the RC-bound HP heme is accompanied by the oxidation of another cyt as shown by the spectral shift (3−4 nm) observed for the light-induced difference spectrum detected 1 ms after the actinic flash in both the γ- and α-band regions (Figure 5). Very similar results were obtained for cells of *Rvi. gelatinosus* strains ATCC 17011 and TG9 grown under dark aerobic conditions (data not shown). The simplest interpretation of this behavior is to assume that the RC-bound HP heme is rapidly rereduced by the HP cyt c_8, in agreement with the reconstitution experiments of Matsuura et al. (*14*). It can be estimated, from the relative amplitudes of the light-induced absorbance changes detected at 50 μs and 1 ms, that about 80% of the photooxidized RC-bound HP heme is rereduced by the soluble HP cyt c_8, consistent with the amount of this cyt per RC. The comparable contribution of the photooxidized HP cyt c_8 and of the photooxidized RC-bound HP heme at 422 nm explains why the electron donation between these two electron carriers does not induce significant variations in the light-induced changes (Figure 3). The rate of electron transfer between the HP cyt c_8 and the photooxidized RC-bound HP heme can be measured at 416.5 nm, an isosbestic point in the difference spectrum of the photooxidized RC-bound HP heme (Figure 5). The halftime of this reaction was 400 μs (inset of Figure 5). This rate is very similar to the rate of electron transfer between HiPIP and photooxidized RC-bound HP heme for cells of *Rvi. gelatinosus* grown under PS conditions (Figure 3). It is therefore difficult to know whether the fast phase of small amplitude observed at 422 nm for dark aerobically grown cells (Figure 3) is linked to a small fraction of HP interacting with the HiPIP or to a small difference in extinction coefficient for the RC-bound HP heme and HP cyt c_8.

DISCUSSION

We have shown by redox titration that the periplasmic fractions of three different strains of *Rvi. gelatinosus* contain a soluble high midpoint potential cyt, named HP cyt c_8, in addition to LP cyt c_8. This finding contrasts with the commonly accepted view. This cyt was characterized in more detail from strain IL144. This cyt can be readily separated from the LP cyt c_8 with the help of a CM-23 column. The E_m of the HP cyt c_8 was 300 mV, i.e., 270 mV higher than the value determined for the LP cyt c_8 and 30 mV lower

than that of the HiPIP. The HP and LP cyts c_8 also differed in their molecular masses, 9470 and 9433 Da for the HP cyt c_8 and the LP cyt c_8 (*22*), respectively, and in their amino acid sequences (Table 1). The molecular mass of HP cyt c_8 and its amino acid sequence indicate that this cyt is a cyt c_8. The HP cyt c_8 is present in small quantities for cells grown under anaerobic photosynthetic conditions but its synthesis is enhanced 4−6-fold for dark aerobically grown cells. The small amount of this cyt in cells grown under photosynthetic condition and the difficulty distinguishing it from the LP cyt c_8 in gel electrophoresis experiments probably explains why it was not found in several previous studies. In the case of *Marichromatium* (formerly *Chromatium*) *purpuratum*, Kerfeld et al. (*27*) also reported difficulties separating low and high midpoint potential cyts *c* of low molecular mass by SDS−PAGE. On the other hand, our observation accounts for some reports of a HP cyt *c* in different *Rvi. gelatinosus* strains. Already in 1983, Senn and Wüthrich (*28*) found two small isocyts *c*-551 in the periplasm of *Rvi. gelatinosus* 29−1. They did not succeed in purifying either of them by electrophoresis and chromatographic techniques, but deduced from NMR experiments that their midpoint potential differed by more than 120 mV. The homology between the N-terminal sequence of one of the isocyt *c* of *Rvi. gelatinosus* 29−1 and that determined for the HP cyt c_8 of *Rvi. gelatinosus* IL144 is very high (Table 1). Matsuura et al. (*14*) described the isolation of a soluble cyt *c* from cells of *Rvi. gelatinosus*. Like horse cyt *c*, this cyt was able to reduce the photooxidized RC-bound HP heme. Recently, Borsari et al. (*15*) characterized the redox properties of a cyt *c* isolated from *Rvi. gelatinosus* DSM 1709 in detail. By cyclic voltammetry and spectroelectrochemical titration, they determined a midpoint potential of 294 mV at pH 7. These authors propose that the marked difference between this midpoint potential and that previously measured (+30 mV) in the soluble fraction of *Rvi. gelatinosus* may be due to the binding of $Fe(CN)_6^{3-}$ used as oxidant in the previous studies. A simpler explanation would be that this strain of *Rvi. gelatinosus* also contains both high and a low midpoint potential cyts *c* that have been successfully separated by this group.

Amino acid sequences characteristic of cyts c_8 have been determined for different periplasmic electron carriers present in several phototrophic organisms that contain an RC-bound tetraheme cyt. This is the case for *Rhodocyclus (Rcy.) purpureus*, *Rcy. tenuis* (*8*), *Allochromatium* (formerly *Chromatium*) *vinosum* (*29*), *Marichromatium purpuratum* (*27*), and *Rhodoferax (Rfx.) fermentans* (*30*). Although cyts c_8 occur mostly in the nonphotosynthetic pseudomonas and in *Azotobacter vinelandii* (*4*), the high value of their midpoint potential suggests they could function as secondary electron donors in a manner similar to cyt c_2 in reducing the photooxidized RC (*5*). Experimental evidence for such a role was obtained by flash spectroscopic studies in intact cells of *Allochromatium vinosum* (*31*) and more recently of *Rcy. tenuis* (*26*). In reconstitution experiments using membranes of *Rfx. fermentans*, Hochkoeppler et al. (*30*) found that the cyt c_8 present in this species is able to reduce the RC-bound tetraheme subunit in a fast (sub-ms) and a slow (ms) phase.

In the case of cells of *Rvi. gelatinosus* grown under dark aerobic conditions, clear evidence that the HP cyt c_8 can serve as an electron donor to the photooxidized RC-bound tetraheme cyt is afforded by the spectral shift observed 1 ms after the actinic flash (Figure 5). Its involvement in the photoinduced cyclic electron transfer is attested by the dramatic slowing of its rereduction rate upon addition of stigmatellin, an inhibitor of the cyt bc_1 complex (data not shown). This function is in line with the measured value of its midpoint potential (300 mV). The rate of electron transfer between the HP cyt c_8 and the photooxidized RC-bound HP heme ($t_{1/2}$ = 400 μs) is of the same order of magnitude as those measured for HiPIP ($t_{1/2}$ = 240 μs) (*13*). Similar rates have been measured for the soluble cyt c_8 or cyt c_2 in intact cells of *A. vinosum* ($t_{1/2}$ = 300 μs, *31*), *Rcy. tenuis* ($t_{1/2}$ = 300 μs, *26*), or *Blastochloris* (formerly *Rhodopseudomonas*) *viridis* ($t_{1/2}$ = 110 μs, *32*). Although the HP cyt c_8 can act as electron donor to the photosynthetic reaction center both in vivo for dark aerobically grown cells and in vitro (*14*), its active participation in the photoinduced electron transfer is probably limited to the transition from dark to light growth conditions. Indeed, this cyt is maximally expressed under dark aerobic conditions where its main role is most likely to transfer electrons from the bc_1 complex to a cyt *c* oxidase or analogues of the respiratory chain. Morever, the observation that the gene coding for the HP cyt c_8 is located only 129 bp downstram from an open reading frame coding for a component of a dissimilatory nitrite reductase operon suggests that this cyt could serve also as electron donor in a denitrifying pathway. The ability of HP cyt c_8 to interact with electron carriers of photosynthetic, respiratory, and denitrifying chains is similar to that encountered in several species of photosynthetic bacteria where the cyt c_2 has been shown to be involved in these different bioenergetic processes.

For dark aerobically grown *Rvi. gelatinosus* cells, the HiPIP is in slight excess compared with the HP cyt c_8 (1.3−2 molecules of HiPIP and 0.8−1 HP cyt c_8/RC). Nevertheless, the HP cyt c_8 appears to be the preferential electron donor to the photooxidized RC-bound tetraheme cyt (Figure 5). First and second-order rate contants and binding constant should be determined by measurements of kinetics of electron transfer between purified HiPIP or HP cyt c_8 and reaction center complexes at various concentrations of reactants to precisely characterize this behavior. A detailed phenotypic analysis of mutants deleted in HP cyt c_8 and HiPIP is necessary to unequivocally define the function of these electron carriers in *Rvi. gelatinosus* cells.

ACKNOWLEDGMENT

The authors wish to thank Dr. J. Gaillard for recording EPR spectra and Dr. J. Lavergne for many valuable discussions.

REFERENCES

1. Nitschke, W., and Dracheva, S. M. (1995) in *Anoxygenic Photosynthetic Bacteria* (Blankenship, R. E., Madigan, M. T., and Bauer, C. E., Eds.) pp 775−805, Kluwer Academic, Dordrecht, The Netherlands.
2. Meyer, T. E., and Donohue, T. J. (1995) in *Anoxygenic Photosynthetic Bacteria* (Blankenship, R. E., Madigan, M. T., and Bauer, C. E., Eds.) pp 725−745, Kluwer Academic, Dordrecht, The Netherlands.
3. Ambler, R. P., Daniel, M., Hermoso, J., Meyer, T. E., Bartsch, R. G., and Kamen, M. D. (1979) *Nature 278*, 659−660.
4. Ambler, R. P. (1991) *Biochim. Biophys. Acta 1058*, 42−47.

5. Bartsch, R. G. (1991) *Biochim. Biophys. Acta 1058*, 28−30.
6. Fukushima, A., Matsuura, K., Shimada, K., and Satoh, T. (1988) *Biochim. Biophys. Acta 933*, 399−405.
7. Nitschke, W., Agalidis, I., and Rutherford, A. W. (1992) *Biochim. Biophys. Acta 1100*, 49−57.
8. Ambler, R. P., Meyer, T. E., and Kamen, M. D. (1979) *Nature 278*, 661−662.
9. Osyczka, A., Yoshida, M., Nagashima, K. V. P., Shimada, K., and Matsuura, K. (1997) *Biochim. Biophys. Acta 1321*, 93−99.
10. De Klerk, H., and Kamen, M. D. (1966) *Biochim. Biophys. Acta 112*, 175−178.
11. Tedro, S. M., Meyer, T. E., and Kamen, M. D. (1976) *J. Biol. Chem. 251*, 129−136.
12. Meyer, T. E. (1970) Ph.D. Dissertation, University of California, San Diego.
13. Schoepp, B., Parot, P., Menin, L., Gaillard, P., Richaud, P., and Verméglio, A. (1995) *Biochemistry 34*, 11736−11742.
14. Matsuura, K., Fukushima, A., Shimada, K., and Satoh, T. (1988) *FEBS Lett.* 237, 21−25.
15. Borsari, M., Benini, S., Marchesi, D., and Ciurli, S. (1997) *Inorg. Chim. Acta 263*, 379−384.
16. Hoshino, Y., and Satoh, T. (1985) *Agric. Biol. Chem. 49*, 3331−3332.
17. Clayton, B. J., and Clayton, R. K. (1978) *Biochim. Biophys. Acta 501*, 470−477.
18. Uffen, R. L. (1976) *Proc. Natl. Acad. Sci. 73*, 3298−3302.
19. Sabaty, M., Gagnon, J., and Verméglio, A. (1994) *Arch. Microbiol. 162*, 335−343.
20. Thomas, P. E., Ryan, D., and Lewin, W. (1976) *Anal. Biochem. 75*, 168−176.
21. Nagashima, K. V. P., Matsuura, K., Wakao, N., Hiraishi, A., and Shimada, K. (1997) *Plant Cell Physiol. 38*, 1249−1258.
22. Igarashi, N., Shimada, K., Matsuura, K., and Nagashima, K. V. P. (1998) in *Photosynthesis: Mechanisms and Effects* (Garab, G., Ed.) pp 2889−2892, Kluwer Academic, Dordrecht, The Netherlands.
23. Kawasaki, S., Arai, H., Kodama, T., and Igarashi, Y. (1997) *J. Bacteriol. 179*, 235−242.
24. Arai, H., Sanbongi, Y., Igarashi, Y., and Kodama, T. (1990) *FEBS Lett. 261*, 196−198
25. Zannoni, D. (1989) *Biochim. Biophys. Acta 975*, 299−316.
26. Menin, L., Schoepp, B., Garcia, D., Parot, P., and Verméglio, A. (1997) *Biochemistry 36*, 12183−12188.
27. Kerfeld, C. A., Chan, C., Hirasawa, M., Kleis-SanFransisco, S., Yeates, T. O., and Knaff, D. B. (1996) *Biochemistry 35*, 7812−7818.
28. Senn H., and Wüthrich, K. (1983) *Biochim. Biophys. Acta 743*, 69−81.
29. Samyn, B., De Smet, L., Van Driessche, G., Meyer, T. E., Bartsch, R. G., Cusanovich, M. A., and Van Beeumen, J. J. (1996) *Eur. J. Biochem. 236*, 689−696.
30. Hochkoeppler, A., Ciurli, S., Kofod, P., Venturoli, G., and Zannoni, D. (1997) *Photosynth. Res. 53*, 13-21.
31. Van Grondelle, R., Duysens, L. N. M., Van der Wel, J. A., and Van der Wal, H. N. (1977) *Biochim. Biophys. Acta 461*, 188−201.
32. Garcia, D., Richaud, P., and Verméglio, A. (1993) *Biochim. Biophys. Acta 1144*, 295−301.

BI991146H